SCEC 2006 Annual Report

Interseismic strain near San Bernardino and Coachella Valleys constrained by InSAR

Submitted by David Schmidt and Beth Wisely
Department of Geological Sciences
12722 University of Oregon
Eugene, OR 97403-1272

INTRODUCTION

We have developed a method for estimating the vertical component of tectonic deformation in aquifer basins occurring at fault bends and junctures along the southern San Andreas fault system. A goal of this project is to contribute meaningful estimates of interseismic vertical strain rates as additional geodetic constraints in the existing fault slip rate models. Our method involves a least-squares inversion, using both InSAR and well level time series. We invert for the vertical tectonic displacement rate and a poroelastic coefficient at each well site. Herein, we critically examine initial results for systematic biases and fallibilities in the technique.

METHOD

Data

We have processed hundreds of interferograms for both the Upper Coachella Valley and the San Bernardino basin. Most of these InSAR images are dominated by the non-tectonic deformation signals caused from hydraulic changes within these extensively managed aquifer basins. In order to better resolve the tectonic vertical displacement fields for the Coachella Valley and San Bernardino basin, the hydrologic contribution to the deformation needs to be removed. In the majority of tectonic geodetic studies, the vertical component of displacement is ignored in part due to biases from non-tectonic sources. The use of only horizontal components of displacement is typically sufficient given that the San Andreas fault system is a transpressive plate boundary dominated by strike-slip motion. However, some vertical deformation is expected over the long term, as evidenced by the high regional topographic relief. Vertical deformation is also expected during the interseismic period at fault bends, fault junctions, and locations where the interseismic slip rate changes [e.g. *McClay and Bonora*, 2001; *Bilham and King*, 1989; *Crowell*, 1974].

Model

We propose a method, which we call the Interferometric Hydrogeologic Inversion Technique (IHIT), in which a time series of well depth-to-water measurements can be used as a means of removing the hydrologically induced surface deformation signal from the InSAR data. Fluctuations in head levels result from the natural and anthropogenic cycles of groundwater recharge to the aquifers, and can produce a poroelastic response as the sediment matrix expands and contracts elastically. Permanent land subsidence can result from extensive periods of aquifer overdraft and the subsequent compaction of fine sediment and clays. As this permanent compaction occurs on the order of decades [*Poland and Davis*, 1969], we assume the short period deformation observed with InSAR is dominantly elastic.

We suggest that the vertical surface deformation inferred from InSAR represents the combined effects of groundwater fluctuations and tectonic motion. Here we assume that the range-change signal reflects vertical ground motion. In reality, there is also a horizontal component of displacement related to fault parallel motion. We have removed a gradient from each interferogram, which filters out this horizontal component to first order. The seasonal fluctuation in the pore pressure should mirror surface deformation allowing us to estimate the poroelastic coefficient and the hydrologically induced deformation (Figure 1). The remaining trend should reflect tectonic motion. Using the surface deformation inferred from InSAR and head level changes inferred from well water levels, we invert for the elastic coefficient at well sites, and the vertical tectonic deformation rate. We assume the InSAR data and well level data are related as,

$$I(\vec{x},t) = k(\vec{x})w(\vec{x},t) + u(\vec{x})t + c \qquad (1)$$

where $I(\vec{x},t)$ is the InSAR time series at a well location $\vec{x}$, $\mathrm{k}(\vec{x})$ is the poroelastic coefficient related to the compressibility of the sediments [*Riley,* 1969], $w(\vec{x},t)$ is the well level time series, $u(\vec{x})$ is the vertical tectonic displacement rate at the well location, and *c* is a constant. This model assumes that a well level time series reflects the effective pore pressure change through the aquifer. We formulate this problem as a least squares inversion, $Gm = d$, and solve for the model parameters where,

$$m = \text{ model parameters } = \begin{bmatrix} k(\vec{x}) & u(\vec{x}) & c \end{bmatrix}^{\mathrm{T}}$$

$$d = \text{ data } = \begin{bmatrix} I(\vec{x},t) \end{bmatrix}$$

$$G = \text{ design matrix } = \begin{bmatrix} w(\vec{x},t) & t & 1 \end{bmatrix}.$$

Since the InSAR data and well level data are sampled at different times, we interpolate the well data linearly or by fitting a sinusoid.

RESULTS

InSAR

We have carefully scrutinized the temporal and spatial patterns of deformation for the Coachella Valley and San Bernardino basin using various InSAR analysis techniques. In the Coachella Valley (Figure 2a), the radar phase is coherent over the majority of the upper valley (Indio to San Gorgonio Pass). Ascending track interferometry reveals that the dominant direction of displacement observed in the Coachella Valley from 1992-2000 is vertical. Near Indio we observe an oblong shaped region of land subsidence with a maximum average subsidence rate of 8-9 mm/yr from 1993-2000. In the northwest corner of the valley, near the Whitewater Recharge facility, InSAR measures a maximum average uplift rate of 3-4 mm/yr for the same time span. InSAR time series derived using the technique of *Schmidt and Bürgmann* [2003] reveal a prominent transient seasonal deformation signal throughout the basin. In general, areas of inferred subsidence correlate with decreasing aquifer head levels, and areas of uplift correlate with increasing head levels, suggesting that the observed surface deformation in the Coachella Valley is related to pore pressure changes in the underlying sediment [e.g. *Schmidt and Bürgmann*, 2003]. Another observation supporting that there is a significant hydrologic component to surface deformation is in the northwest corner of the Coachella Valley where we observe a pattern of differential surface uplift across the sub-parallel Garnet Hill and Banning faults. Maximum relative uplift is observed south of the Garnet Hill fault, near the Whitewater Recharge facility, where groundwater recharge elastically expands the surrounding sedimentary matrix. Uplift decreases to the north across each fault by ~1.5-2.0 mm/yr, presumably due to the faults acting as semi-permeable barriers to groundwater flow. We are currently working with colleagues to model this groundwater flow across the Garnet Hill and Banning faults as an extension of this work.

Interferometry for the San Bernardino basin (Figure 2b) also appears to be dominated by a vertical deformation signal, although we have not yet processed ascending track data for this area. Assuming that the range change signal reflects vertical deformation, we infer a maximum uplift rate of 3 mm/yr from 1995-2000, with localized regions of subsidence in the Lytle Creek and Santa Ana River drainages. Unlike the Coachella Valley, seasonal fluctuations in the InSAR time series are not observed in the San Bernardino basin. However, seasonal fluctuations can be observed in some of the San Bernardino well time series. *Lu and Danskin* [2001] examined InSAR data prior to 1995, and suggest that observed surface deformation was correlated to variations in storm runoff and aquifer recharge from year to year. To help understand the lack of a seasonal signal in the San Bernardino InSAR observations, we look to refine our InSAR time series data set, and to investigate the complexities of the regional groundwater system. Due to the complex basin structure [*Anderson et al*., 2004] and extensive groundwater withdrawal, the San Bernardino basin is susceptible to disequilibrium in hydraulic head [*Danskin and Freckleton*, 1992]. Techniques to regain hydraulic equilibrium include the above-ground transport of water for recharge from areas with anomalously high water tables to the alluvial recharge facilities. This artificially sustained near-surface groundwater transport may interrupt or mask any seasonal surface displacement signal related to the deeper aquifer system.

Model Estimates

The displacement rates mentioned above are average rates derived from stacked differential interferograms, and presumably represent the combined effects of hydrology and tectonics. To remove hydrologic effects from the observed displacements, we use the IHIT method previously described, incorporating the time dependent surface displacements and groundwater level fluctuations. For sites located in the subsiding region of the Upper Coachella Valley (Figure 2a), IHIT produced a range of *tectonic subsidence* rates of 1.7-6.7 mm/yr. These rates are consistent with published estimates for tectonic basin subsidence [*Dorsey and Umhoefer*, 2000; *Itoh et al.,* 2000; *Takano*, 2001; *Bilham and King*, 1989]. Near the Whitewater recharge facility where InSAR measures relative uplift IHIT estimates a range of *tectonic uplift* rates of 0.7-3.3 mm/yr. Inferred tectonic uplift in the San Gorgonio Pass is supported by the facts that the pass lies within a restraining bend geometry of the San Andreas fault zone, and that transpressional structures, like the Garnet Hill, are in close proximity to the region of maximum estimated uplift.

Tectonic uplift rates for the San Bernardino basin (Figure 2b) are estimated at 1.6 mm/yr at the wells west of the San Jacinto fault (Rialto-Colton sub-basin), and 1.0 mm/yr at the wells east of the San Jacinto fault. Well data for the localized subsiding regions (Lytle Creek and Santa Ana River drainages) were not available at the time of our initial processing run, and we currently have no estimate for tectonic displacement rates in these two areas.

INTERPRETATION

We have considered several approaches to ascertaining the validity of the initial results from IHIT. The model parameters themselves can be used to assess whether the inversion technique produces reasonable estimates. Firstly, the poroelastic coefficient, $k(\vec{x})$, is equivalent to the classic aquifer mechanics term S_{ke}, or the elastic deformation of the aquifer system skeleton [e.g.

Poland and Davis, 1969]. S_{Ske} is the component of average specific storage due to elastic deformation and is calculated by scaling $k(\bar{x})$ (or S_{ke}) to the aquifer thickness at the given well site, $d(\bar{x})$.

$$S_{Ske} = k(\bar{x})/d(\bar{x}) \qquad (2)$$

Anderson et al. [2004] published a map of basin depth for the San Bernardino area, which we incorporated into the S_{Ske} calculations. We compare our S_{Ske} model estimates to those of other aquifer studies as a test of the consistency of our method. Figure 3 shows a graphical comparison of S_{Ske} values from this study to those of other published aquifer studies. S_{Ske} values calculated for the San Bernardino basin are in excellent agreement with those from previous studies. The significantly broader range of S_{Ske} values for the Coachella Valley is likely an artifact of limited information on aquifer thickness and basin depth [*Reichard and Meadows*, 1992]. Better constraints on aquifer thickness/basin depth may decrease variability of S_{Ske} values among the well locations for the Upper Coachella Valley.

The second model parameter estimated with IHIT, $u(\bar{x})$, is the vertical tectonic displacement rate. As mentioned, tectonic subsidence rate estimates fell within estimates from previous studies of tectonic basin subsidence. However, these results varied through the valley with no obvious spatial pattern. Also, the tectonic rate estimates consistently correlate to the direction of total deformation observed with InSAR. This poses a question. Will IHIT be able to correctly resolve a situation in which a basin is tectonically subsiding but experiencing aquifer recharge such that InSAR measures surface uplift? Alternately, would IHIT be able to resolve a tectonically uplifting region that is experiencing aquifer overdraft such that InSAR measures land subsidence? IHIT can be tested for this type of sensitivity through random sampling of false data sets that mimic each of the situations described above.

To further hone the results produced using IHIT, we require better spatial coverage of well locations and detailed well site characterizations (e.g. well bottom depth, perforation depth, and stratigraphic composition). Such characterization can lend insight as to whether a well accesses the entire aquifer column and adequately represents pore pressure changes throughout the aquifer system. We have recently shifted the primary focus of this investigation from the Coachella Valley to the San Bernardino basin for two main reasons. The first reason is the high-resolution basin structure for San Bernardino by *Anderson et al.* [2004]. Secondly, we have developed a working relationship with a Geographic Information Systems expert at the San Bernardino Valley Municipal Water District who has retrieved over 1000 well site depth-to-water level archives and site characterizations throughout the San Bernardino and Rialto-Colton basins, providing us with an opportunity to fully test IHIT and ascertain uncertainties of the method. This incorporation of new San Bernardino well sites is an on-going project for which we expect results in the coming months.

The IHIT method produces plausible estimates of elasticity and tectonic deformation where the well data is correlated with the InSAR data. Surface displacement appearing anti-correlated with groundwater levels suggests that these particular well sites inaccurately represent pore pressure changes through the aquifer column. The IHIT method is not applicable to well sites that access only perched or semi-perched upper-most aquifer layers. Future work includes the incorporation of estimated vertical tectonic displacement rates into modeling of the interseismic and long-term deformation along the southern San Andreas fault system.

REFERENCES

Anderson, Megan, Jonathan Matti, Robert Jachens [2004], Structural model of the San Bernardino basin, California, from analysis of gravity, aeromagnetic, and seismicity data, *J. Geophys. Res., vol. 109, B04404*, doi:10.1029/2003JB002544.

Bilham, Roger, and Geoffrey King [1989], The Morphology of Strike-Slip Faults: Examples from the San Andreas Fault, California, *J. Geophys. Res., vol. 94, no. B8*, 10,204-10,216.

Crowell, John C. [1974], Origin of late Cenozoic basins in southern California, *Special Publication – Society of Economic Paleontologists and Mineralologists, vol. 22,* 190-204.

Danskin, W. R., John R. Freckleton [1992], Ground-water flow modeling and optimization techniques applied to high-ground-water problems in San Bernardino, California: U.S. Geological Survey Water-Supply Paper W2340, 165-177.

Dorsey, Rebecca J., and Paul Umhoefer, 2000, Tectonic and eustatic controls on sequence stratigraphy of the Pliocene Loreto basin, Baja California Sur, Mexico: *GSA Bulletin, v. 112, no. 2,* 177-199.

Itoh, Yasuto, Keiji Takemura, Tatsuya Ishiyama, Yukari Tanaka, Hirome Iwaki, 2000, Basin formation at a contractional bend of a large transcurrent fault: Plio-Pleistocene subsidence of the Kobe and northern Osaka Basins, Japan: *Tectonophysics 321*, 327-341.

Lu, Z., and W. R. Danskin [2001], InSAR analysis of natural recharge to define structure of a ground-water basin, San Bernardino, California, Geophys. Res. Lett., 28, 2661-2664.

McClay, Ken, and Massimo Bonora [2001], Analog models of restraining stepovers in strike-slip fault systems: *AAPG Bull., vol. 85, no. 2,* 233-260.

Poland, J. F., and G. H. Davis [1969], Land subsidence due to withdrawal of fluids, *Rev. Eng. Geology, 2*, 187-269.

Reichard, Eric G., Kevin Meadows [1992], Evaluation of a ground-water flow and transport model of the Upper Coachella Valley, California: U.S. Geological Survey Water-Resource Investigations Report 91-4142, p. 101.

Riley, F.S. [1969], Analysis of borehole extensometer data from central California: *Land Subsidence, vol.2, edited by L.K. Tison, Int. Assoc. Sci. Hydrol. Pub., 89*, 423-431.

Schmidt, David A., and Roland Bürgmann, [2003], Time-dependent land uplift and subsidence in the Santa Clara valley, California, from a large Interferometric synthetic aperture radar data set, *J. of Geophysical Research*, vol.108, no., B9, doi:10.1029/2002JB002267.

Takano, O., 2001, Changes in depositional systems and sequences in response to basin evolution in a rifted and inverted basin: an example from the Neogene Niigat-Shin'etsu basin, Northern Fossa Magna, central Japan: *Sedimentary Geology 152*, 79-97.

FIGURES

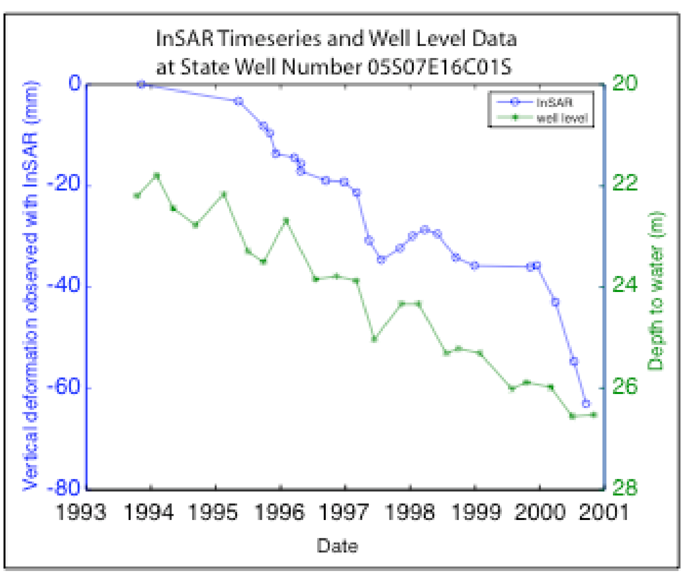

Figure 1. InSAR time series (in blue) at the location of State Well Number 05S07E16C01S (see figure 2a) plotted with depth to water (in green). Graphing of each data set uses a linear interpolation between each data point and may not represent the total range of vertical deformation or water level. The plotted data show rough short and long-term correlation with similar peaks, troughs, and general trend through time. This type of plot is the basis for the IHIT method.

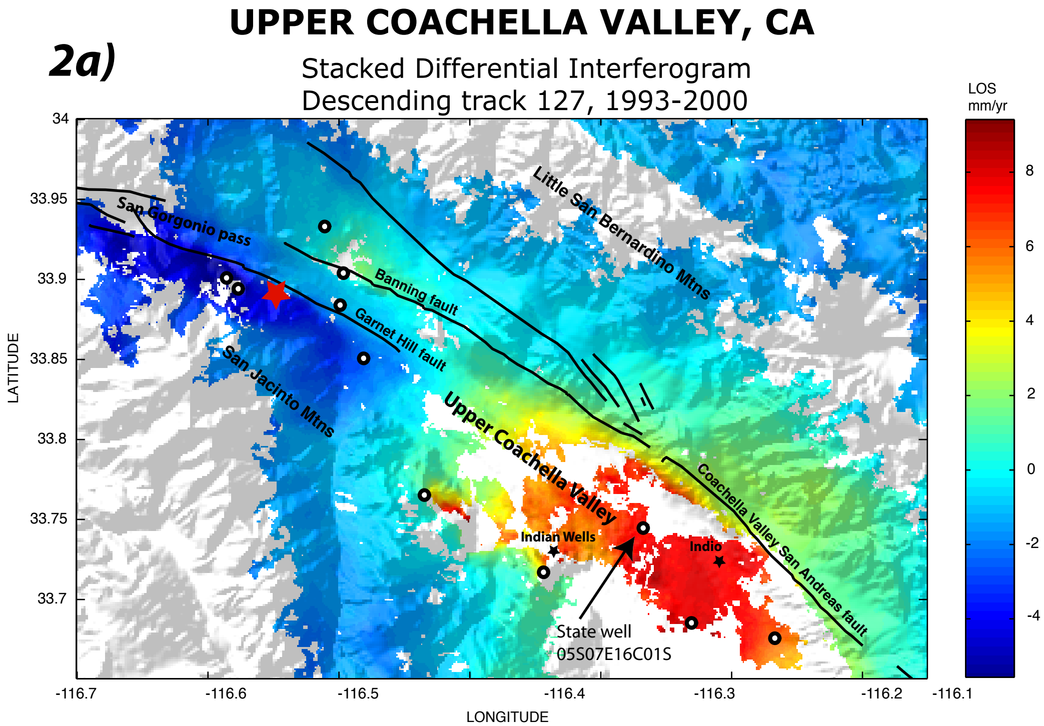

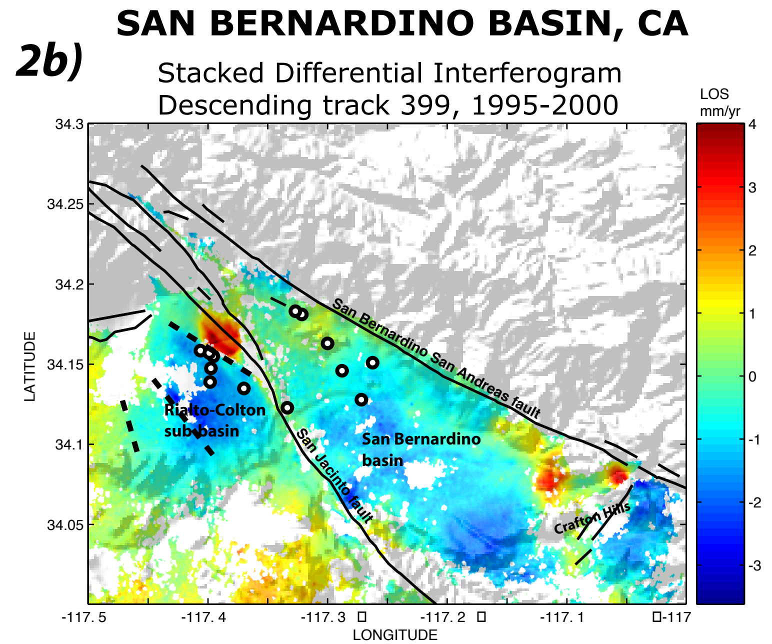

Figure 2. Stacked differential interferograms measuring satellite line-of-sight range change in mm/yr. Images are superimposed on shaded relief. Positive range change indicates motion away from the satellite, and negative range change indicates motion towards the satellite. Regions with no color are uncorrelated regions where we have no data. Individual interferograms were chosen for their good spatial coherence and minimal atmospheric contamination. Black lines are regional faults. Dotted black lines are groundwater barriers observed with InSAR timeseries. Black circles are well sites used in the initial run of HIT. The red star is the Whitewater Recharge Facility. The Coachella Valley stack, 2a, is composed of 23 individual interferograms with an average baseline of 74m. The San Bernardino stack, 2b, is composed of 30 individual interferograms with an average baseline of 65m.

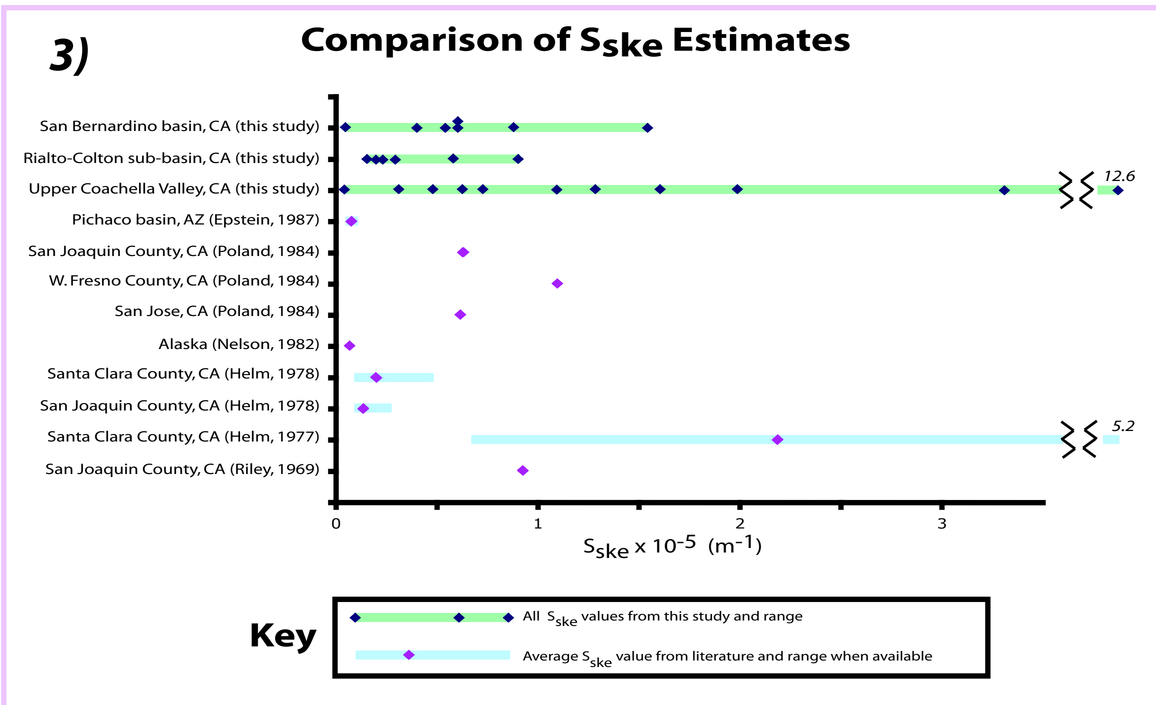

Figure 3. Graphical comparison of S_{ske} estimates. Green bars represent the range of results from this study, with blue a blue diamond for each value. Pale blue bars represent the range of results from other studies, with a purple diamond for the average value. Purple diamonds with no range bar are averages given with no accompanying range.